EFFECT OF ELECTRON-BEAM MELTING AND HEAT TREATMENT ON THE STRUCTURE, COMPOSITION, AND PROPERTIES OF TOOL STEELS

A. I. Veinik, I. L. Pobol',
and A. A. Shipko

UDC 621.365.91:537.533

A method was developed for the surface-melting and quench-hardening of tool steels through the use of electron-beam heating. The distribution of alloying elements in characteristic treatment zones was studied.

Tool steels for use in cold deformation must have high wear resistance, strength, and hardness in combination with toughness and heat resistance. Die steels for use in hot-working must in addition have good resistance to crazing and scaling at high temperatures and good thermal conductivity [1]. The ductility, impact toughness, and strength of alloy steels are affected to a significant extent by the content of gases and nonmetallic inclusions in the metal [2]. Insufficiently high ductility properties are one of the main reasons for low crack resistance in die steels. One consequence of this is the removal of dies from service due to crazing at high temperatures. Crazing is a particular problem in the use of molds for die casting.

From thirty to 75% of the nonmetallic inclusions in steels are removed in electron-beam (EB) remelting. Optimum EB remelting regimes provide for reductions in the contents of oxide, sulfide, and nitride inclusions by a factor of 1.5-10 compared to metal made by an open process. For example, the content of oxide inclusions is reduced by a factor of 4-10 [3]. The distribution of nonmetallic inclusions is made more uniform and the inclusions are made more disperse. Coarse stringer-type inclusions in the structure of the initial metal are converted into globular inclusions and the size of the oxide inclusions is reduced. It follows from the literature data [3, 4] that the EB remelting of metals and alloys significantly increases the complex of physico-mechanical properties in the steel. In tool steels, there is an increase in density and impact toughness and a reduction in the susceptibility to hot-cracking [5].

Analysis of the literature shows that the EB method is used mainly for treating ingots of metals. There is almost no research data on the use of the method as one of the processes in the concluding stage of production of the original metal. There have not been any studies of the features of the transformations which occur in steels and alloys under such heating conditions, nor has anyone investigated the effect of different types of heat treatment on the structure, composition, and properties of the treated products.

In connection with this, we established the goal of studying the structural transformations, composition, and properties of die steels 5KhNM, 4Kh5MFS, and DI23, and ball-bearing steel ShKh15SG after surface melting by the EB method. We also sought to develop methods to subsequently improve the structure and properties of tool steels through their heat treatment.

To solve these problems, it was necessary to develop a method of experimentally investigating the EB melting of steel semifinished products that would permit determination of the effect of heating parameters on the temperature field of the specimens and the depth of melting.

We studied the effect of the scanning frequency, power, and time of action of the electron beam on the temperature distribution in the test steels. Here, we used cylindrical specimens 70-90 mm in diameter and 6-35 mm high. Holes 2.5 mm in diameter were drilled to different depths parallel to the specimen axis for the insertion of thermocouples. The placement of the thermocouples allowed us to obtain a complete picture of the temperature distribution in the specimen during its treatment. Temperature curves describing the heating were recorded on ÉPP-09MZ potentiometers. The power of the beam during EB melting was

Physicotechnical Institute, Academy of Sciences of the Belorussian SSR, Minsk. Translated from Inzhenerno-Fizicheskii Zhurnal, Vol. 54, No. 1, pp. 121-129, January, 1988. Original article submitted September 1, 1986.

0022-0841/88/5401-0095 $12.50

TABLE 1. Content of Alloying Elements in Steels, %, in the Initial State and after EB Melting (EBM)

Grade of steel	Condition of steel	C	Si	Mn	Cr	W	V	Mo	Ni
DI23	Initial	0,49	0,62	0,56	2,61	3,24	1,51	0,79	—
	After EBM	0,49	0,62	0,21	2,46	3,36	1,66	0,90	
5KhNM	Initial	0,58	0,28	0,61	0,71	—	—	0,17	1,80
	After EBM	0,56	0,26	0,22	0,71	—	—	0.17	1,65
4Kh5MFS	Initial	0,36	0,80	0,27	5,25	—	0,56	1,50	—
	After EBM	0,40	0,80	0,10	5,25	—	0,56	1,50	—
ShKh15SG	Initial	0,98	0,58	1,15	1,46	—	—	—	—
	After EBM	1,00	0,56	0,36	1,50	—	—	—	—

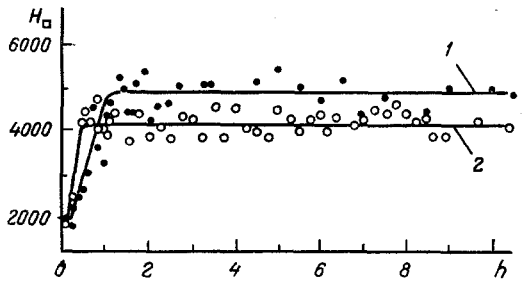

Fig. 1. Distribution of microhardness in the surface layer of steel 4Kh5MFS after EB melting; acceleration voltage 10 kV, beam current 90 mA, bath holding time 540 sec (1) and 300 sec (2), depth of molten zone 8.5 (1) and 7.1 mm (2), respectively. $H_□$, MPa.

varied from 800 W to 1500 W by changing the current and accelerating voltage. The specific power was 50-2600 W/cm². The beam was swung over a rectilinear section of the surface at frequencies in the range 200-600 Hz, the sides of the rectangle measuring from 5 to 40 mm. The time the metal was held in the molten state ranged from 300 to 540 sec. The holding time was reckoned from the moment that melting began. At the end of the holding period, the specific power of the beam was gradually reduced to zero. We simultaneously reduced the amplitude of the sweeps. The inclusions in the steel rose toward the surface during the holding period and were displaced into the last zone of metal subjected to EB heating by the crystallization front formed during directional solidification.

Study of the temperature field in the tool-steel specimens showed that with the use of optimum values of scanning frequency, the temperature front moves into the depth of the specimen parallel to the heating surface. An increase in EB heating power during the initial period of treatment increases the temperature gradient in the cross section of the specimen. For all heating regimes, the temperature distribution in this section is described by a parabolic law. However, the curvature of the parabola decreases with an increase in heating time and the value of n in the below equation (1) approaches unity. An increase in beam power shortens the time required to reach the steady state during heating of a given specimen. These laws, obtained from semifinished products corresponding to acutal small parts, can be applied in the treatment of parts of any size.

The melting depth in the semifinished products was calculated in relation to energy density and the time of action of the electron beam by using the method of separation of variables [7]. In accordance with this method, the temperature distribution in the product can be approximated by the equation of a parabola of the degree n:

$$T = (T_s - T_i)(y/X)^n + T_i. \quad (1)$$

The melting process begins at $t = t_1$, when the depth of the liquid region $\xi = 0$. The process lasts until the moment $t = t_2$, when the required melting depth is reached. The heat-balance equation can be represented in the form

$$dQ_{e\ell} = dQ_{ac} + dQ_{rad} + dQ_{cr}. \quad (2)$$

The components of the heat balance correspond to elementary quantities of heat transmitted by the electron beam with the specific power $q_{e\ell}$ over an area F. This heat is accumulated in a planar body of the thickness L and is expended on phase transformations during melting and evaporation:

$$dQ_{e\ell} = q_{e\ell} F dt; \quad (3)$$

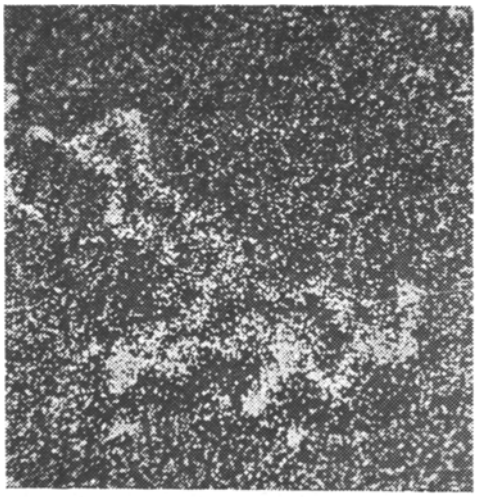

Fig. 2

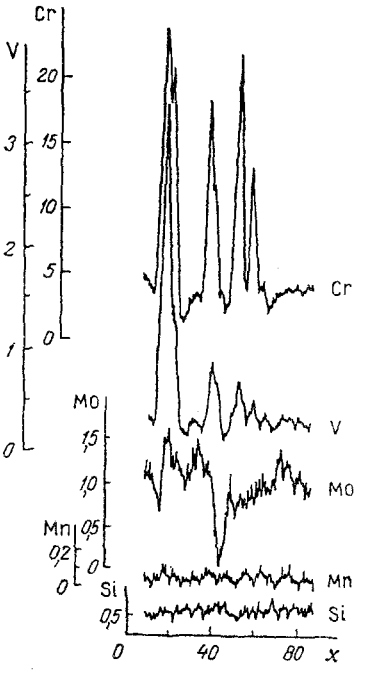

Fig. 3

Fig. 2. Image of scanned region in characteristic CrK_α-radiation of steel 4Kh5MFS in the inclusion concentration zone with EB melting of inclusions.

Fig. 3. Distribution of alloying elements, %, in steel 4Kh5MFS in the inclusion concentration region produced by EB melting (the scanned section is shown in Fig. 2).

$$dQ_{ac} = \frac{\lambda n}{L} (T_{cr} - T_i) F dt; \tag{4}$$

$$dQ_{cr} = \rho r F d\xi; \tag{5}$$

$$dQ_{rad} = C (T^4_{cr} - T^4_d) F dt. \tag{6}$$

After substitution of (3)-(6) into Eq. (2), integration yields the relation

$$\xi = \frac{1}{\rho r} [q_{el} - C (T^4_{cr} - T^4_d) - \frac{\lambda n}{L} (T_{cr} - T_i)] (t - t_1). \tag{7}$$

This relation can be used for engineering calculations of the depth of the molten zone.

It is known [8] that with a sufficiently long holding time (1-9 min), nonmetallic inclusions rise to the surface and are either removed in the gas phase or remain on the surface in the form of slag. A study of nonmetallic inclusions in treated steels conducted by means of Nanolab 7 and Omnicon FAS II microscopes showed a reduction in total nonmetallic inclusion content in the EB melting region by a factor of 1.6-6.6 compared to the initial state. The inclusions were also significantly refined. For example, the average area of one inclusion in steel 5KhNM decreased by a factor of 7.3. These results agree with the findings in [3-5]. Figure 1 shows the character of the distribution of microhardness $H_\square$ in the surface layer of steel 4Kh5MFS after EB melting. It is evident from the graph that the depth of the region with a reduced microhardness increases with an increase in the time of holding of the melt from 300 to 540 sec. This is evidence of the large accumulation of nonmetallic inclusions in the surface layers, which must be considered when deciding on the final mechanical shaping of the treated products.

Table 1 shows results of chemical analysis of the composition of the steels in the initial state and after EB melting. It is evident from the table that the manganese content

TABLE 2. Microhardness of the Axes of Dendrites ($H_{\square}^{a}$) and Interaxial Zones ($H_{\square}^{i}$) and the Degree of Dendritic Segregation K_D of the Steels after EB Melting

Steel	Microhardness, MPa		K_D, %
	$H_{\square}^{i}$	$H_{\square}^{d}$	
4Kh5MFS	8630	7780	10,9
5KhNM	6120	3390	80,5
DI23	7670	6020	27,4
ShKh15SG	5020	4640	8,2

undergoes the greatest reduction (by 63-70%), while the content of vanadium, molybdenum, and tungsten increases somewhat.

Using steels 4Kh5MFS and 5KhNM as examples, we resorted to x-ray spectral analysis to study the distribution of alloying elements in the initial and fused parts of the specimen and the region to which the inclusions migrate. In each case, we analyzed micrographs of the test sections, their images in absorbed electrons, and images obtained in the corresponding characteristic radiations – VK_{α}, MoK_{α}, etc. The darker sections on the images in absorbed electrons correspond to the predominance of elements with a large atomic number. In these cases, the x-ray images were obtained by means of the scanning system of the microprobe. A semi-quantitative evaluation of the distribution of the analyzed element in the images obtained in characteristic radiations was made in accordance with the density of luminous points on the micrographs.

As an example of the images obtained, Fig. 2 shows the image produced in characteristic CrK_{α}-radiation of the inclusion concentration region in steel 4Kh5MFS. Figure 3 shows the quantitative distribution of the alloying elements. The studies revealed that the analyzed section of the specimen contains many inclusions and that the concentrations of chromium and vanadium undergo the greatest changes around these inclusions. At the boundaries of the inclusions, the content of these elements decreases to 2 and 0.2%, respectively, and it exhibits a large gradient relative to the dark sections within the inclusion itself (13-23 and 3.5%). The content of silicon and manganese in the test section of the specimen remains constant – including within the inclusion – and, as will be shown below, coincides with the melting section.

Analysis of the distribution of alloying elements in the initial zone – characterized by a structure of temper martensite with traces of the deformed structure along the rolling axis – showed that the main alloying elements (chromium, molybdenum, vanadium, manganese) are distribured unevenly in the microvolumes. The greatest concentration gradients (vanadium from 1.8-2.8 to 0.3%, chromium from 5 to 10%, molybdenum from 1.5 to 25%) are related to an increased content of their compounds along the remaining traces of deformation. The distribution of silicon is uniform.

In the fused region, rid of most of its inclusions, the silicon concentration remains constant. This region is characterized by a dendritic structure and a low content of small, light inclusions. The manganese content is equalized over the entire volume and is reduced to 0.05% as a result of its partial vaporization (high value of vapor density). This finding is consistent [9] with study of the chemical composition by the spectral method. At the same time, the gradients in the concentrations of chromium, vanadium, and molybdenum remain substantial in the microvolumes – the sites of inclusions which did not dissolve and did not float to the surface during melting.

It can be seen from the above results that the EB melting of steels is accompanied by purification of the metal, producing increases in impact toughness, thermal conductivity, and scaling resistance. At the same time, the structure formed during solidification of the molten steel is characterized by dendritic segregation and coarse grains. In steels 4Kh5MFS, 5KhNM, and DI23, the first-order axes of the dendrites are located roughly perpendicular to the interface between the molten and solid metal along directions of intensive heat removal during crystallization. No distinct dendrites were found in steel ShKh15SG after melting.

We studied (under a load of 0.981 N) the microhardness of the axes of dendrites ($H_{\square}^{a}$) and interaxial zones ($H_{\square}^{i}$) enriched with alloying elements. The values obtained are shown in Table 2. We used the relation

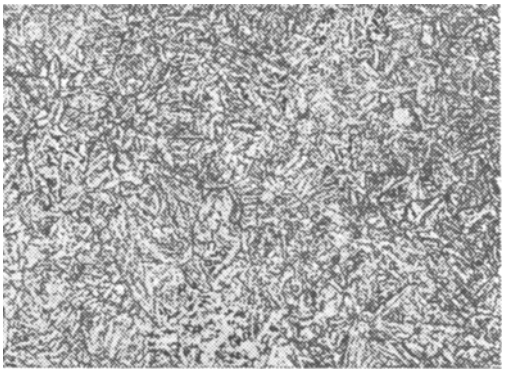

Fig. 4. Microstructure of steel 4Kh5MFS after EB melting, diffusion annealing, annealing for grain refinement, quenching with moderate tempering, and EB surface-hardening, × 500.

$$K_D = (H^i_\square - H^d_\square)/H^d_\square \cdot 100\,\%$$

to calculate the degree of dendritic segregation of the steel after EB melting. Of the steels investigated, steel 5KhNM exhibited the greatest amount of such segregation, while steels 4Kh5MFS and ShKh15SG exhibited the least.

Such a structure prevents the material from benefitting fully from EB melting in regard to the possible improvement in service characteristics.

To eliminate these undesirable structural features, we tried used different types of heat treatment. Die (4Kh5MFS, 5KhNM, DI23) and ball-bearing (ShKh15SG) steels were subjected to EB melting following by diffusion annealing, annealing to a fine grain size, and EB surface-hardening. Performing the operations in this sequence made possible to significantly refine the grains of all of the steels and impart a high surface hardness. The depth of the hardened zone depended on the duration of EB heating during the last operation.

It was found that the tool steels are harder after such a combination treatment than after the traditional treatment — bulk quenching and tempering. For example, after EB surface-hardening and low-temperature self-tempering, steels 5KhNM, 4Kh5MFS, and DI23 reach hardnesses HRC_e equal to 64-66, 57-58, and 55-56, respectively. This can be attributed to the EB purification of the surface zone, diffusional equalization of the composition of the steel during homogenization, and refinement of the grain during EB surface-hardening. X-ray microanalysis of the distribution of alloying elements in the strengthened layers of steels 4Kh5MFS and 5KhNM showed that their concentrations in steel 5KhNM, for example, are Mo 0.2%, Cr 0.7%, Ni 1.0%, and Mn 0.1%. Figure 4 shows the microstructure of steel 4Kh5MFS heat-treated by the above-described combination method of surface-hardening.

One way of increasing the durability of tool steels for hot-deforming is reducing their thermal stresses, the magnitude of which depends in large part on the thermal conductivity of the steels. According to [10], the life of molds for die casting is inversely proportional to the temperature of its surface and the thermal stresses. An increase in thermal conductivity can be achieved by EB melting of the steels. This was shown in [11] in a study of the effect of the regimes of EB melting on thermal conductivity. The latter increases with an increase in test temperature. After EB melting, thermal conductivity is increased by 21-43% for steel 5KhNM, 12-27% for steel 4Kh5MFS, up to 13% for steel DI23, and by 29-49% for steel ShKh15SG. The exact increase depends on the test temperature. This pattern of increase is attributable not only to the removal of nonmetallic inclusions, gases, and impurities dissolved in the steels during the melting operation, but also to a 60-70% reduction in the content of Mn in the steel (Mn has a low thermal conductivity) and a moderate increase in the relative content of elements with a high thermal conductivity (V, Mo, W).

A new technology for making products of tool steels was developed on the basis of the experimental data. The technology includes EB melting of the initial semifinished product in the working sections of a part, diffusion annealing, annealing to a fine grain, shaping of the surface without a machining allowance, and a concluding EB surface-hardening. By being cleaned of nonmetallic inclusions and gases during melting, the steel acquires a homogeneous martensitic structure which is very hard. The increased hardness of the surface layer, combined with the improved ductility of the refined metal and the greater thermal conductivity and scaling resistance of the steel, results in an improvement in the service characteristics of products made by this method. It is best to use this technolgy to make tools — in particular, dies for hot-working. Such products can be subjected to higher temperatures

without reducing th eir strength properties. Commercial trials of molds for die casting made by the proposed method showed that the resistance of the tool to crazing is 20% greater than for dies made by the traditional method of bulk quenching.

NOTATION

n, exponent of the approximating parabola; T, temperature of the body in an arbitrary plane; T_s, specimen surface temperature; T_i, initial temperature; T_{cr}, melting point of the heated material; T_a, ambient temperature; y, distance from the symmetry axis of the parabola to the plane with arbitrary temperature; X, thickness of the layer heated to the moment of time t; t, arbitrary time; t_1, time to beginning of melting of surface; ξ, depth of liquid zone; t_2, time to melting of specimen to a specified depth; dQ_{el}, quantity of heat transmitted by the electron beam; dQ_{ac}, quantity of accumulated heat; Q_{rad}, quantity of heat lost by radiation; Q_{cr}, quantity of heat expended on melting; q_{el}, specific power of the electron-beam heating; L, thickness of the plane body; ρ, density of the heated material; r, heat of fusion of the material; C, radiation coefficient; λ, thermal conductivity; $H_{\square}$, microhardness; K_D, degree of dendritic segregation; F, heating area; h, distance from the surface; x, linear size of the scanned section.

LITERATURE CITED

1. Yu. A. Geller, Tool Steels [in Russian], Moscow (1975).
2. M. I. Vinograd, Inclusions in Steel and Its Properties [in Russian], Moscow (1963).
3. B. E. Paton, B. I. Medovar, D. A. Dudko, et al., Problems of Steel Ingots [in Russian], Moscow (1974), pp. 43-53.
4. M. Val'ster, A. Shuderi, and K. Forkh, Chern. Met., No. 22, 22-33 (1968).
5. O. F. Antropov, S. I. Tishaev, L. A. Pozdnyak, et al., Manufacture and Study of High-Speed and Die Steels [in Russian], Moscow (1970), pp. 129-134.
6. A. I. Veinik, V. F. Alekhin, I. L. Pobol', and V. L. Bondarenko, Inventor's Certificate No. 908851, "Method of surface heat treatment of products," Byull. Izobret., No. 8 (1982).
7. A. I. Veinik, Approximate Calculation of Heat-Conduction Processes [in Russian], Moscow—Leningrad (1959).
8. A. L. Tikhonovskii and A. A. Tur, Refining of Metals and Alloys by Electron-Beam Melting [in Russian], Kiev (1984).
9. I. L. Pobol' and A. A. Shipko, Distribution of Alloying Elements in the Electron-Beam Melting of Tool Steels, Submitted to VINITI 17.07.86, No. 5230-B.
10. A. I. Batyshev, E. M. Bazilevskii, V. I. Bobrov, et al., Stamping of Molten Metal [in Russian], Moscow (1979).
11. G. V. Markov and I. L. Pobol', Vestsi Akad. Nauk BSSR, Ser. Fiz. Tekh. Nauk, No. 2, 23-25 (1985).

GROUP ANALYSIS OF THE HEAT-CONDUCTION EQUATION IN DISPLACEMENTS OF ISOTHERMAL SURFACES. 2. OBTAINING INVARIANT SOLUTIONS OF BOUNDARY-VALUE PROBLEMS

N. M. Tsirel'man

UDC 536.24.01

A rule is formulated and examples are given for constructing particular solutions of boundary-value problems of heat conduction.

The present paper is a development of the results [1] referring to obtaining invariant solutions for the equation of the nonstationary heat-conduction process

$$x'_\tau = f(T)\, x''_{TT}\, (x'_T)^{-2} - f'(T)\, (x'_T)^{-1}, \tag{1}$$

written for the location x of isothermal surfaces T = idem at the time τ. The function f(T) in (1) is related to the temperature dependences of the heat-conduction coefficient $\lambda(\tilde{T})$ and

Sergo Ordzhonikidze Ural Aviation Institute. Translated from Inzhenerno-Fizicheskii Zhurnal, Vol. 54, No. 1, pp. 129-133, January, 1988. Original article submitted October 14, 1986.

0022-0841/88/5401-0100 $12.50